Authors

Maria A. Navarro, Alfonso Saiz-Lopez, Carlos A. Cuevas, Rafael P. Fernandez, Elliot Atlas, Xavier Rodriguez-Lloveras, Douglas Kinnison, Jean Francois Lamarque, Troy Thornberry, Andrew Rollins, James W. Elkins, Eric J. Hintsa, and Fred L. Moore

Atmospheric
Chemistry
and Physics

Modeling the inorganic bromine partitioning in the tropical tropopause layer over the eastern and western Pacific Ocean

Maria A. Navarro[1], **Alfonso Saiz-Lopez**[2], **Carlos A. Cuevas**[2], **Rafael P. Fernandez**[3], **Elliot Atlas**[1],
Xavier Rodriguez-Lloveras[2], **Douglas Kinnison**[4], **Jean-Francois Lamarque**[4], **Simone Tilmes**[4], **Troy Thornberry**[5,6],
Andrew Rollins[5,6], **James W. Elkins**[5], **Eric J. Hintsa**[5,6], and **Fred L. Moore**[5,6]

[1]Department of Atmospheric Sciences, RSMAS, University of Miami, Miami, Florida, USA
[2]Department of Atmospheric Chemistry and Climate, Institute of Physical Chemistry Rocasolano, CSIC, Madrid, Spain
[3]National Research Council (CONICET), FCEN-UNCuyo, UTN-FRM, Mendoza, Argentina
[4]Atmospheric Chemistry Observations & Modeling Laboratory, National Center for Atmospheric Research,
Boulder, Colorado, USA
[5]National Oceanic & Atmospheric Administration, Earth System Research Laboratory, Boulder, Colorado, USA
[6]Cooperative Institute for Research in Environmental Science, University of Colorado, Boulder, Colorado, USA

Correspondence to: Maria A. Navarro (mnavarro@rsmas.miami.edu)

Abstract. The stratospheric inorganic bromine (Br_y) burden arising from the degradation of brominated very short-lived organic substances (VSL_{org}) and its partitioning between reactive and reservoir species is needed for a comprehensive assessment of the ozone depletion potential of brominated trace gases. Here we present modeled inorganic bromine abundances over the Pacific tropical tropopause based on aircraft observations of VSL_{org} from two campaigns of the Airborne Tropical TRopopause EXperiment (ATTREX 2013, carried out over the eastern Pacific, and ATTREX 2014, carried out over the western Pacific) and chemistry-climate simulations (along ATTREX flight tracks) using the specific meteorology prevailing. Using the Community Atmosphere Model with Chemistry (CAM-Chem) we model that BrO and Br are the daytime dominant species. Integrated across all ATTREX flights, BrO represents ~ 43 and 48 % of daytime Br_y abundance at 17 km over the western and eastern Pacific, respectively. The results also show zones where Br / BrO > 1 depending on the solar zenith angle (SZA), ozone concentration, and temperature. On the other hand, BrCl and $BrONO_2$ were found to be the dominant nighttime species with ~ 61 and 56 % of abundance at 17 km over the western and eastern Pacific, respectively. The western-to-eastern differences in the partitioning of inorganic bromine are explained by different abundances of ozone (O_3), nitrogen dioxide (NO_2),

total inorganic chlorine (Cl_y), and the efficiency of heterogeneous reactions of bromine reservoirs (mostly $BrONO_2$ and HBr) occurring on ice crystals.

1 Introduction

The role of bromine in stratospheric ozone depletion has been discussed in several studies (Brinckmann et al., 2012; Daniel et al., 1999; Fernandez et al., 2017; Hossaini et al., 2015; Prather and Watson, 1990; Salawitch et al., 2005; Sinnhuber et al., 2009; Wofsy et al., 1975). Many of these discuss the contribution of brominated very short-lived organic substances (VSL_{org}) like bromoform ($CHBr_3$), dibromomethane (CH_2Br_2), bromochloromethane (CH_2BrCl), dibromochloromethane ($CHBr_2Cl$), and bromodichloromethane ($CHBrCl_2$), in addition to long-lived halons and methyl bromide, as an important source of stratospheric bromine. The reaction mechanisms of VSL_{org} that lead to the formation of inorganic bromine (Br_y) involve complex sets of reactions that have been described in previous modeling studies (Krysztofiak et al., 2012; Ordóñez et al., 2012; Hossaini et al., 2010). The chemistry is initiated mainly via reaction with OH and by photolysis and leads to the formation of several unstable organic halogenated radi-

cals. The fate of these radicals, and their mechanisms of reaction, is controlled by NO_x conditions and OH levels. In polluted environments (high-NO_x regime), the radicals react to produce NO_2 or halogenated nitrates that can decompose, experience oxidation or photolysis, and washout or react on surfaces. In "clean" environments (low-NO_x regime), the radicals undergo a series of cross reactions (including reaction with HO_2) leading to the formation of several different products that can continue reacting with OH (or Cl), washout, or photodissociate to form Br_y species as the end product (Krysztofiak et al., 2012).

The implementation of the complex chemistry of very short-lived species in current models like the Community Atmospheric Model with Chemistry (CAM-Chem) has been simplified by assuming that Br_y is immediately formed from photo-oxidized VSL_{org} (Ordóñez et al., 2012). However, the challenge to simulate VSL_{org} observations and to quantify their degradation products ($Br_y = Br + BrO + HOBr + BrONO_2 + HBr + BrCl + 2Br_2 + BrNO_2$) relies on other atmospheric processes that could modify this chemistry. For example, the location and timing of emissions, the transport dynamics and dehydration processes in the tropical tropopause layer (TTL) (Liang et al., 2010), and the occurrence of heterogeneous recycling reactions on sea-salt aerosol and ice crystals (Fernandez et al., 2014) affect the total amount of inorganic bromine that can be injected into the stratosphere. A recent study by Navarro et al. (2015), which examined the TTL over the Pacific Ocean, showed the impact of strong convective events on the chemistry of brominated species. The estimates of the contribution of very short-lived substances to total stratospheric bromine over the tropical eastern and western Pacific showed a similar amount of VSL_{org} over both regions. Nevertheless, a smaller amount of Br_y was observed over the western Pacific due to the influence of the South Pacific Convergence Zone (SPCZ) and the path of typhoon Faxai in 2014.

As tropical circulation, assisted by convection, could enhance the vertical transport of VSL_{org}, the VSL_{org} degradation products could reflect changes in their abundances and chemical speciation. A previous study by Fernandez et al. (2014) calculated that VSL_{org} provided an annual average tropical stratospheric injection of total bromine of approximately 5 ppt (parts per trillion), where ~ 3 ppt entered the stratosphere as a product gas, while ~ 2 ppt entered as a source gas. In the Fernandez et al. (2014) study, the distribution of Br_y species showed Br and BrO to be the dominant inorganic species during daytime, particularly over the tropical western Pacific, which they suggested was a hot spot with increased stratospheric bromine injection (~ 3.8 ppt Br_y and ~ 3.8 ppt VSL_{org}). This study also introduced the concept of the "tropical ring of atomic bromine", a photochemical phenomenon that extends in the tropics from approximately 15 to 19 km, where the abundance of Br atoms is favored due to low temperatures (less than 200 K) and low O_3 abundances (less than 100 ppb). Similarly, the estimates of stratospheric

Br_y inferred from measurements of BrO during the NASA Airborne Tropical TRopopause EXperiment (ATTREX) deployment over the eastern Pacific showed approximately 3 to 5 ppt Br_y for potential temperatures between 350 and 400 K in the TTL (Werner et al., 2017). These previous studies, as well as many others (e.g., Dorf et al., 2008; Brinckmann et al., 2012; and Liang et al., 2010), highlighted the importance of Br_y product gas transportation from the lower troposphere into the TTL and lower stratosphere as well as its impact on ozone.

Our study focuses mainly on the difference in modeled Br_y concentrations in the TTL over the Pacific throughout the ATTREX campaign flight tracks, and examines temporal and spatial distributions of Br_y. Based on the reliable representation of the observed VSL_{org} by the CAM-Chem model (Navarro et al., 2015) and to further investigate the chemistry of bromine tracers in the TTL, we estimated the partitioning of Br_y over the tropical eastern and western Pacific during 2013 and 2014, respectively. From this case study analysis, we also complement the study of the diurnal Br_y speciation in the TTL and the Br / BrO ratio distribution in the upper troposphere–lower stratosphere (UTLS) modeled by Fernandez et al. (2014) and Saiz-Lopez and Fernandez, (2016).

This paper is organized as follows: Sect. 2 briefly describes the campaign, the methods used for the observations of trace gases, and the characteristics of the model simulations. Section 3 discusses the major findings regarding the amount of Br_y and its partitioning within the TTL, as well as its relevance for the formation of the proposed tropical ring of atomic bromine (Fernandez et al., 2014; Saiz-Lopez and Fernandez, 2016). In addition, Sect. 3 discusses the results of a sensitivity test in the model where water–ice aerosol reactions are deactivated. Section 4 summarizes and concludes this study.

2 Methods

2.1 Observations

2.1.1 ATTREX campaign

ATTREX, an airborne campaign focused on the chemical and physical processes in the TTL (~ 13–18 km altitude), took place over the Pacific Ocean during boreal winter (Jensen et al., 2015). Details of the instruments, the flights, and collected data for the NASA-ATTREX mission can be found in Jensen et al., (2015). In 2013, six flights were conducted over the eastern and central Pacific, targeting the area between 187 to 268° E and 11° S to 34° N (hereafter referred to as the eastern Pacific, EP). In 2014, eight flights were conducted over the western Pacific, covering the area between 120 to 165° E and 11° S to 35° N (hereafter referred to as the western Pacific, WP). On board the NASA Global Hawk, the University of Miami deployed the Global Hawk Whole Air

Sampler (GWAS) to collect more than 900 samples at different locations along the flight tracks. From these measurements, 436 observations along the flight track (388 during the day and 48 at night) over the WP and 309 flight points (152 during the day and 157 at night) over the EP were used to simulate Br_y partitioning (Fig. 1). Due to the logistics of the missions, the distribution of sample points according to the solar zenith angle (SZA) was different between the WP and EP. During ATTREX 2014 (WP), flights occurred mostly during daylight hours as the plane took off in the early local morning ($\sim 17{:}00$ UTC, $03{:}00$ LT). Also, flights lasted approximately 20 h, which reduced the amount of nighttime samples, particularly at high SZA. The flight tracks were oriented in different directions, mostly west–east and north–south, and even a local circle flight, following a different path departing from and returning to Andersen Air Force Base ($13.5°$ N, $144.9°$ E). For these reasons, samples showed a high density of observations at $50°$ SZA and no observations beyond $130°$ SZA for the WP. In contrast, during ATTREX 2013 (EP) flights also took off during early morning ($\sim 15{:}00$ UTC, $07{:}00$ LT), but lasted between 22 and 24 h. In addition, the flight tracks were oriented in southern and southwestern direction and returned to Edwards Air Force Base ($34.9°$ N, $243.8°$ E) over the same path. Hence for the EP, the number of samples was evenly distributed along the entire range of SZAs.

2.1.2 VSL$_{org}$ observations

Measurements of VSL$_{org}$ were carried out with the GWAS during the deployments and were used here to evaluate the model. Detailed methodology and implementation of this instrument is described in Navarro et al. (2015). Briefly, the GWAS contained 90 custom-made 1.3 L stainless steel canisters with electrically operated solenoid valves. Two metal bellows pumps (Senior Aerospace) flow ambient air through a custom inlet at 2 to $8 L min^{-1}$ depending on the altitude. The instrument is fully automated and controlled from the ground through an Ethernet interface. During the ATTREX mission, samples were collected along the Global Hawk flight track at different altitudes by closing the exhaust valves (Parker Hannifin) and opening the solenoid valve (Parker Hannifin) of the selected sample canister. When the desired pressure was reached, the canister valve was closed and the manifold continued flushing. After sample collection, canisters were analyzed using a high-performance gas chromatograph (Agilent Technology 7890A) and mass spectrometer with mass selective, flame ionization, and electron capture detectors (Agilent Technology 5975C).

The VSL$_{org}$ bromine budget and the vertical distribution of these species were presented in Navarro et al. (2015), which also included estimates of the organic vs. inorganic bromine fraction over the EP and WP. At the tropopause level (~ 17 km), the modeled estimates of the organic bromine fractions derived from very short-lived species were sim-
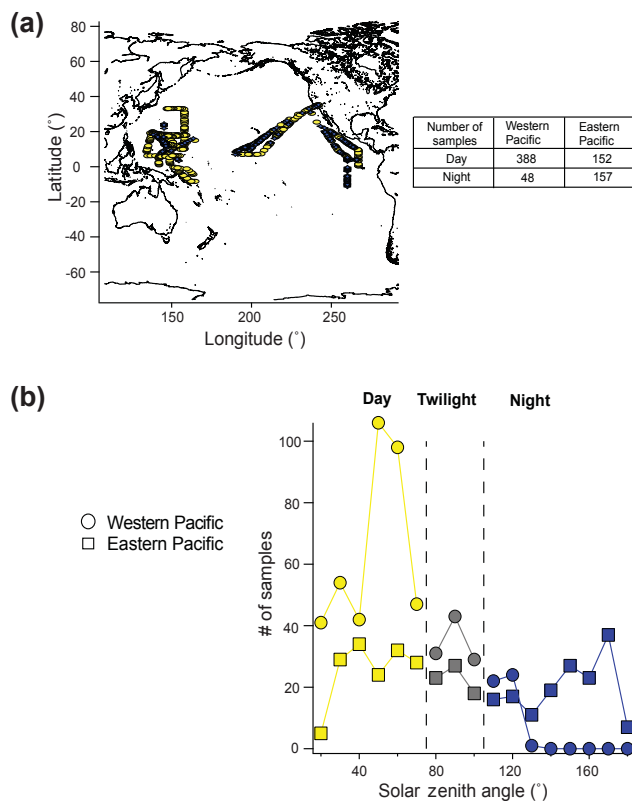

Figure 1. (a) Location of GWAS observations along ATTREX flight tracks taken at different altitudes over the WP and EP. Yellow filled circles represent the samples taken during the day and blue filled circles the samples taken at night. **(b)** Sample density of GWAS observations arranged by solar zenith angle over the western and eastern Pacific. Yellow filled circles represent samples taken over the WP during daylight, while blue filled circles are the samples taken over the WP during nighttime. Yellow filled squares represent the samples taken over the EP during daylight, while blue filled squares are the samples taken over the EP during nighttime. Grey circles and squares are the samples taken during twilight over the WP and EP, respectively.

ilar for the entire Pacific (3.84 ± 0.64 and 3.18 ± 1.49 ppt from the WP and EP, respectively). However, the inorganic fraction inferred from VSL$_{org}$ measurements showed 3.02 ± 1.90 ppt of Br_y over the EP and 1.97 ± 0.21 ppt over the WP (Navarro et al., 2015). Based on these results, we performed model simulations to look into the variability and distribution of the Br_y partitioning. To evaluate the model we also used ozone concentrations measured with the National Oceanic and Atmospheric Administration's Ozone system (NOAA-O$_3$) during ATTREX 2013, and the Unmanned aircraft system Chromatograph for Atmospheric Trace Species (UCATS-O$_3$) during ATTREX 2014.

2.1.3 O_3 observations

Measurements of ozone were carried out with dual-beam UV photometers. These instruments utilize two identical absorption cells, a mercury lamp, an ozone scrubbing catalyst, and two detectors that measure 253.7 nm UV radiation transmitted through the absorption cell. At this wavelength, the ozone absorption cross section is well known, and thus the ozone number density can be readily calculated by Beer's law. Since the two absorption cells are identical, virtually continuous measurements of ozone are made by alternating the ambient air sample and the ozone-scrubbed sample between the two cells. At a fast collection rate (from 2 Hz at < 200 hPa to 0.5 Hz at 500 hPa for NOAA-O_3 and 0.2 Hz for UCATS-O_3), the minimum detectable concentration of ozone corresponds to 1 ppb or less, at standard temperature and pressure. Based on an intercomparison between the two instruments during ATTREX 2013, the UCATS-O_3 instrument was 4.8 ± 0.8 ppb higher than NOAA-O_3 in the concentrations of interest between 50 and 250 ppb, and approached 0 near 500 ppb. The NOAA-O_3 instrument was unavailable on ATTREX 2014. To merge the measurements taken over different timescales, these high-rate measurements of ozone were averaged to match the sample collection times of each GWAS sample ($\sim$ 30–90 s) (Blake et al., 1997, 1999, 2001, 2003, 2004; Schroeder et al., 2014), and then the merged data were compared to CAM-Chem outputs (Kormann et al., 2003; Olson et al., 2012).

2.2 Modeling: CAM-Chem configuration

The estimates of VSL$_{org}$, O_3, and the Br$_y$ partitioning were carried out with the CAM-Chem model, a 3-D chemistry-climate model included with the Community Earth System Model (CESM framework, version 1.1.1) (Lamarque et al., 2012). This model includes a complete photochemistry, wet and dry deposition, and heterogeneous chemistry on sea-salt aerosols and ice particles (Fernandez et al., 2014; Ordóñez et al., 2012). The current setup is based on the bromocarbon emission inventory of Ordoñez et al. (2012), which includes time-dependent geographically distributed sources of $CHBr_3$, CH_2Br_2, CH_2BrCl, $CHBr_2Cl$, $CHBrCl_2$, and CH_2IBr. Here, we do not consider chlorocarbon sources such as CH_2Cl_2 and C_2Cl_4 since those species live long enough to be injected almost entirely as source gases into the stratosphere and contribute little to the tropospheric inorganic chlorine (Cl$_y$) loading (Hossaini et al., 2015); although this situation may change based on current trends (Oram et al., 2017). Additional Br$_y$ and Cl$_y$ sources from sea-salt heterogeneous dehalogenation in the lower troposphere are parameterized (Ordóñez et al., 2012; Fernandez et al., 2014). Prescribed volume mixing ratios of long-lived chlorofluorocarbons (CFCs) and halons at the surface as well as surface concentrations of anthropogenic CO_2, CH_4, N_2O, and other ozone precursors are based on the inventory of Meinshausen

et al. (2011). Global emissions of important ozone precursors (NO_x, CO, and VOCs) were obtained through a harmonization exercise of reactive emissions between the years 2000 and 2005 for different representative concentration pathway (RCP) scenarios (Meinshausen et al., 2011; Lamarque et al., 2011). It is worth noting that all inorganic halogen species (i.e., Cl$_y$ and Br$_y$) are not constrained but explicitly solved at each time step. Losses in CAM-Chem are parameterized following a large-scale precipitation scavenging algorithm that includes a physical treatment of scavenging through improvements in the formulation of the removal in sub-grid-scale cloudy environments. This includes washout as well as ice-phase uptake of soluble inorganic bromine species (each of them with an independent Henry's law constant) within the water column (for details see Neu and Prather, 2012, and Fernandez et al., 2014).

Model simulations were run in specified dynamics (SD) mode using meteorological fields prevailing at the time of the campaigns. A spatial resolution of 1° (longitude) × 1° (latitude) with 56 vertical levels (from the surface to $\sim$ 3.5 hPa) and a temporal resolution of 30 min were used. Model hourly output was sampled at exactly the same times and locations as the ATTREX measurements, without performing either spatial or temporal averaging on model grids. Once each independent flight track was extracted from the model output, all atmospheric quantities were averaged into 1 km altitude bins, standard deviations were calculated, and the model was compared with measured data. The chemistry of Br$_y$ species between day and night was distinguished by disregarding the samples collected during twilight (total solar zenith angle between 80 and 100°). In addition, local estimates of ozone, nitrogen dioxide, and inorganic chlorine concentrations were carried out over the EP and WP along the flight tracks to understand the chemistry that leads to the specific bromine partitioning.

3 Results and discussion

The current modeling study was conducted as part of the work described by Navarro et al. (2015), and it follows the same methodology and statistical analysis for discrete variables. At the time of the model runs and analyses, only ozone and VSL$_{org}$ abundances were available to validate model performance. BrO and NO_2 measurements from the ATTREX mission were not available at the time of this analysis, but have since been published by Werner et al. (2017). Thus, once the model performance during the ATTREX campaign is evaluated in Sect. 3.1, we then proceed to the CAM-Chem modeling case study to determine the Br$_y$ partitioning (Sect. 3.2) and efficiency of heterogeneous recycling reactions (Sect. 3.3) on the mostly unexplored eastern and western Pacific TTL.
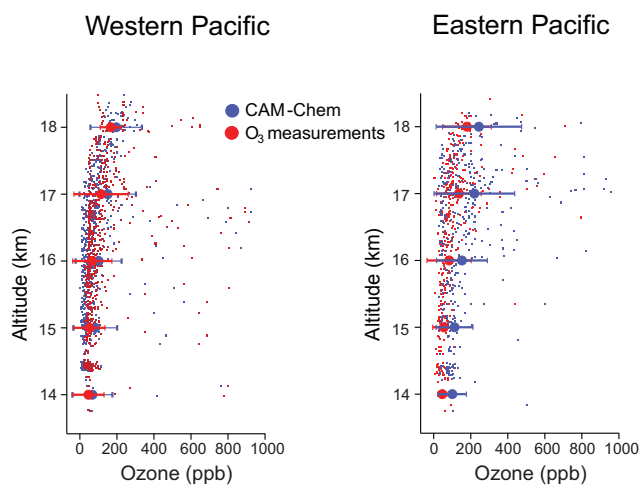
Figure 2. NOAA–UCATS O_3 observations for all flights (blue dots) and CAM-Chem simulations along ATTREX flight tracks (red dots). Filled circles represent the mixing ratios averaged into 1 km altitude bins ±1 SD over the WP and EP to illustrate the altitude variation of ozone. The range of the bins are as follows: 14 km is 13.5–14.5 km, 15 km is 14.5–15.5 km, 16 km is 15.5 –16.5 km, 17 km is 16.5–17.5 km, and 18 km is 17.5–18.5 km. Similar figures for CH_2Br_2 and $CHBr_3$ are in Navarro et al. (2015).

3.1 CAM-Chem model evaluation

The first step of this study was to evaluate the CAM-Chem model chemistry and performance for our intended application. For the evaluation, we used the NOAA-O_3, UCATS-O_3, and organic bromine species from GWAS measurements taken during the ATTREX campaign, since BrO and NO_2 measurements from the ATTREX mission were still under examination by the time of this analysis. Figure 2 shows the measured and model mixing ratios of O_3 in the UTLS for the WP and EP. The NOAA and UCATS O_3 mixing ratios averaged into 1 km altitude bins ranged from 46 to 166 ppb from 14 to 18 km over the WP, and 46 to 179 ppb from 14 to 18 km over EP. CAM-Chem simulations estimated 67 to 196 ppb from 14 to 18 km over the WP, and 100 to 243 ppb from 14 to 18 km over the EP. The model reproduces well the variability of measured ozone with altitude in both the WP and EP. However, the different convective processes are not accurately represented in both regions, which leads to an offset in the EP between measurements and simulated ozone values. The vertical profile of organic bromine species from GWAS measurements can be found in Navarro et al. (2015).

Figure 3 shows the correlation between average measurements and model outputs of the 1 km altitude bins for O_3, $CHBr_3$, and CH_2Br_2 over the WP and EP, as well as the linear regression equations with their associated uncertainties in slopes and intercepts. An excellent correlation ($R^2 > 0.97$) between O_3 measurements and CAM-Chem estimates for both the EP and WP were observed, with slopes not differing significantly from unity. However, small offsets (27.1 ppb in
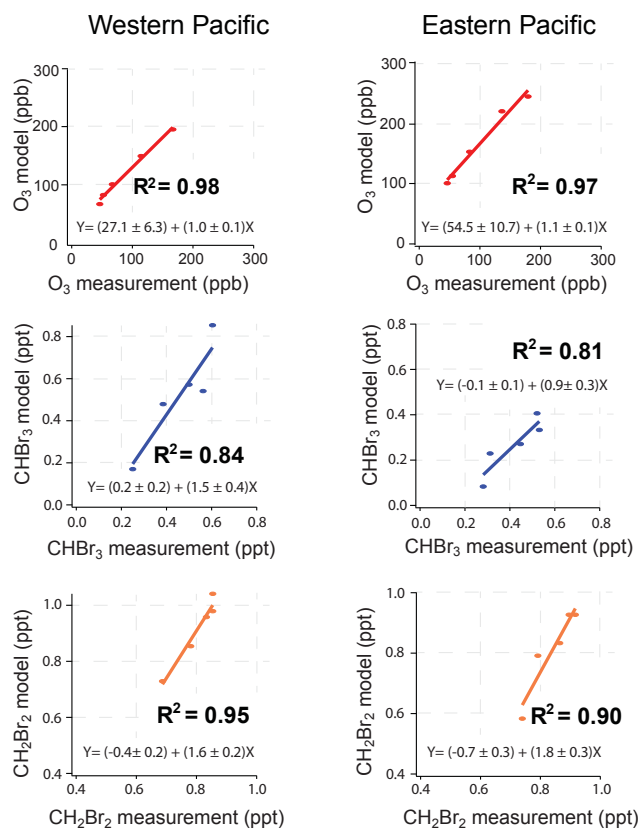
Figure 3. Correlations between measured and modeled mixing ratios of O_3, $CHBr_3$, and CH_2Br_2 over the WP and EP, using 1 km average bins. Filled circles are the mixing ratios averaged into 1 km altitude bins (same as in Fig. 1 for O_3, and Fig. 1 in Navarro et al., 2015, for $CHBr_3$ and CH_2Br_2). Solid lines represent the linear regression analysis of the 1 km average bins including the coefficient of determination (R^2) and regression equation (Y).

the WP and 54.5 ppb in the EP) reflect a bias in the model. In addition, good agreement was observed between GWAS measurements and model simulations of $CHBr_3$ ($R^2 = 0.84$ for the WP; $R^2 = 0.81$ for the EP), and CH_2Br_2 ($R^2 = 0.95$ for the WP; $R^2 = 0.90$ for the EP), as shown in Fig. 3 and the previous work of Navarro et al. (2015).

3.2 Br_y partitioning

The vertical distribution of inorganic species showed a slight variability with altitude (Fig. 4). Over both the WP and EP, BrO and Br are the most abundant species during daytime hours from 14 to 18 km. However, below 16 km the amount of HBr present over the EP tends to be slightly larger than that of atomic Br. For the WP and EP during nighttime hours BrCl and $BrONO_2$ are the dominant species, which is in agreement with Fernandez et al. (2014). Mixing ratios of BrCl closely compete with $BrONO_2$, particularly at 15 and 18 km over the WP. Over the EP, $BrONO_2$ dominates the Br_y species over the entire range of altitudes from 14 to 18 km at
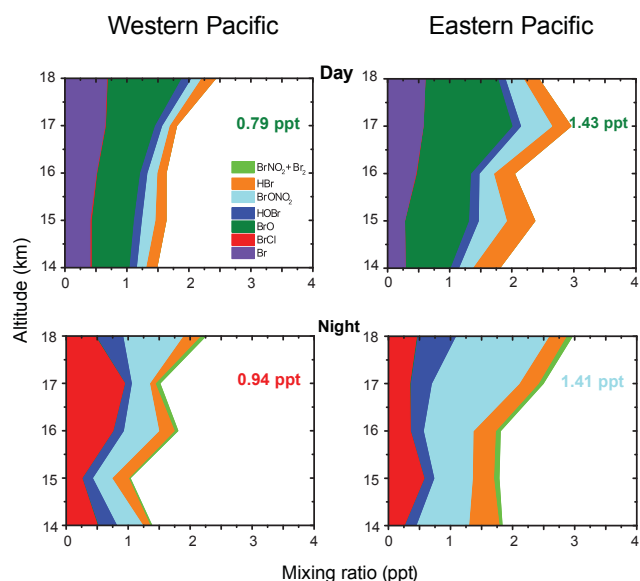
Figure 4. Model calculations of inorganic bromine partitioning along ATTREX flight tracks over the WP and EP using CAM-Chem with prevailing atmospheric conditions (specified meteorology) during the ATTREX campaign. Numbers inside the boxes represent the mixing ratios of BrO (green), BrCl (red), and $BrONO_2$ (light blue) at 17 km.

Table 1. Summary of the CAM-Chem model output of Br_y species at the tropical tropopause level (~ 17 km).

	Species (time)	WP (ppt)	EP (ppt)
Mean	BrO (day)	0.79	1.43
	Br (day)	0.64	0.57
	BrCl (night)	0.94	0.34
	$BrONO_2$ (night)	0.29	1.41
[1]Range	O_3 (day)[2]	35–500	35–900
	NO_2 (day)	1–227	0.7–343
	Cl_y (day)	1–515	1–969
	Temp (day)[3]	188–192	188–206

[1] Range defined as min. and max. values. [2] Units in ppb. [3] Units in K.

night. During daylight hours, the total Br_y burden increases from 1.49 to 2.43 ppt between 14 and 18 km over the WP and from 1.82 to 2.97 ppt over the EP within the same altitude range. Similarly, nighttime Br_y ranges from 1.40 to 2.27 ppt and 1.82 to 2.99 ppt for the WP and EP, respectively. This indicates that the total Br_y atmospheric burden is equivalent within the diurnal cycle. Note that within the same altitude range, the model output for total VSL_{org} decreases from 5.72 ppt at 14 km to 2.53 ppt at 18 km over the WP, and from 3.90 ppt at 14 km to 1.97 ppt at 18 km over the EP, which indicates the dominant role played by very short-lived (VSL) photodecomposition in controlling the Br_y loading in the tropical UTLS (Navarro et al., 2015). Our calculated mean vertical distributions for the EP are at the lower edge of the ranges described by Werner et al. (2017). They report a range for BrO between 0.5 ± 0.5 ppt at the bottom of the TTL and about 5 ppt at potential temperature $\theta = 400$ K, consistent with an inferred increase in Br_y from a mean of 2.63 ± 1.04 ppt to 5.11 ± 1.57 ppt.

At the tropopause level (~ 17 km) and integrated over all flights and SZAs, the inorganic partitioning showed $\sim 43\%$ (0.79 ppt) of abundance of BrO during daylight and $\sim 61\%$ of BrCl (0.94 ppt) during nighttime over the WP. On the other hand, 48% (1.43 ppt) of Br_y is presented as BrO during daylight and 56% (1.41 ppt) as $BrONO_2$ at nighttime over the EP (Fig. 4). Atomic bromine is the second most abundant species during the day, with mean daytime values of 0.64 and 0.57 ppt for the WP and EP, respectively. During the

night, $BrONO_2$ (0.29 ppt) and BrCl (0.34 ppt) are the second most abundant species over the WP and EP, respectively. It is worth noting that even when the maximum inorganic chlorine levels for individual flights are larger in the EP, BrCl is not the dominant nighttime reservoir, while in the WP, where BrCl dominates, the maximum Cl_y mixing ratio is almost half the concentration predicted for the EP (see Table 1 and Figs. 5 and 6). Maximum Cl_y abundances averaged for all flights within each region show less than 85 pptv in the WP and less than 182 pptv for the EP (see Fig. 7), with a global mean tropical annual Cl_y mixing ratio of 50 pptv in agreement with previous reports (Marcy et al., 2004; Fernandez et al., 2014; von Hobe et al., 2011; Jurkat et al., 2014; Mébarki et al., 2010). This can be explained by considering the faster vertical transport occurring in the WP region, which decreases the contribution from photochemical decomposition of VSL chlorocarbons (Saiz-Lopez and Fernandez, 2016). Note that within the TTL, HCl dominates the Cl_y partitioning, with modeled mixing ratios of up to 1 order of magnitude larger than those found for HOCl and $ClONO_2$ (see Fig. 10 in Fernandez et al., 2014). Further knowledge of the complete partitioning between inorganic chlorine species is beyond the scope of this work.

In order to understand the chemistry that led to these modeled abundances, the concentrations of Br_y products (Br, BrO, HOBr, $BrONO_2$, HBr, and BrCl), as well as modeled mixing ratios of the dominant reactants, i.e., O_3, NO_2, and Cl_y, were studied as a function of the SZA for the entire range of altitudes (14 to 18 km). Figures 5 and 6 compare the Br_y partitioning as well as the modeled O_3, NO_2, and Cl_y abundances along all flights in the EP and WP, respectively. Here, it can be clearly observed how the dominant species changes from BrO during daytime to $BrONO_2$ or BrCl during nighttime. Figure 7 shows the mean abundances for all species including all flights in the WP and EP. Even though the mean results do not simulate differences observed in each flight, they do represent and illustrate the average state of the tropical upper atmosphere within the EP
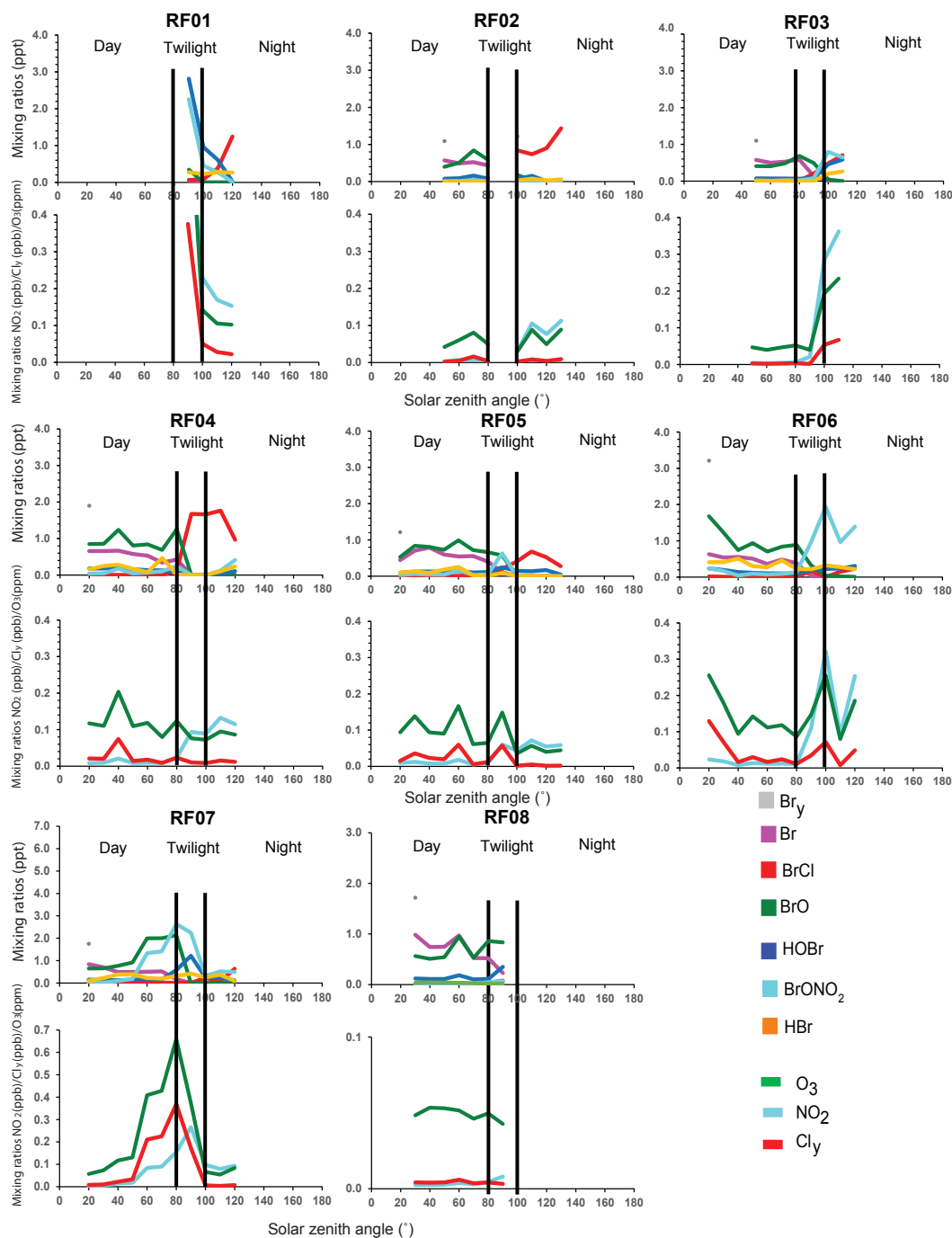
Figure 5. Inorganic bromine species and main reactants of the inorganic chemistry sampled at exactly the same times and locations as the ATTREX flights developed over the western Pacific. Each separated panel shows SZA dependent results for flights RF01, RF03, RF04, RF05, RF06, RF07 and RF08. The black vertical lines represent twilight hours. Only output sampled between 14 and 18 km is considered.

and WP in the presence and absence of sunlight, and should provide relevant information about the dominant processes occurring in each region. During daylight, the high average O_3 (up to ~ 190 ppb) compared to the average Cl_y and NO_2 (Cl_y up to ~ 84 ppt, NO_2 up to ~ 33 ppt) (Fig. 7) led to the rapid formation of BrO over the WP (Fig 7a). As the

SZA increases, a decrease in photolysis (particularly at SZAs of ~ 100–$120°$, Fig. 7b) allows the heterogeneous reaction of inorganic chlorine (mostly HCl) and bromine reservoirs (HOBr and $BrONO_2$) to increase the production of BrCl during the night. Note that the accumulation of nighttime BrCl is more evident during ATTREX 2014 due to larger ice-crystal
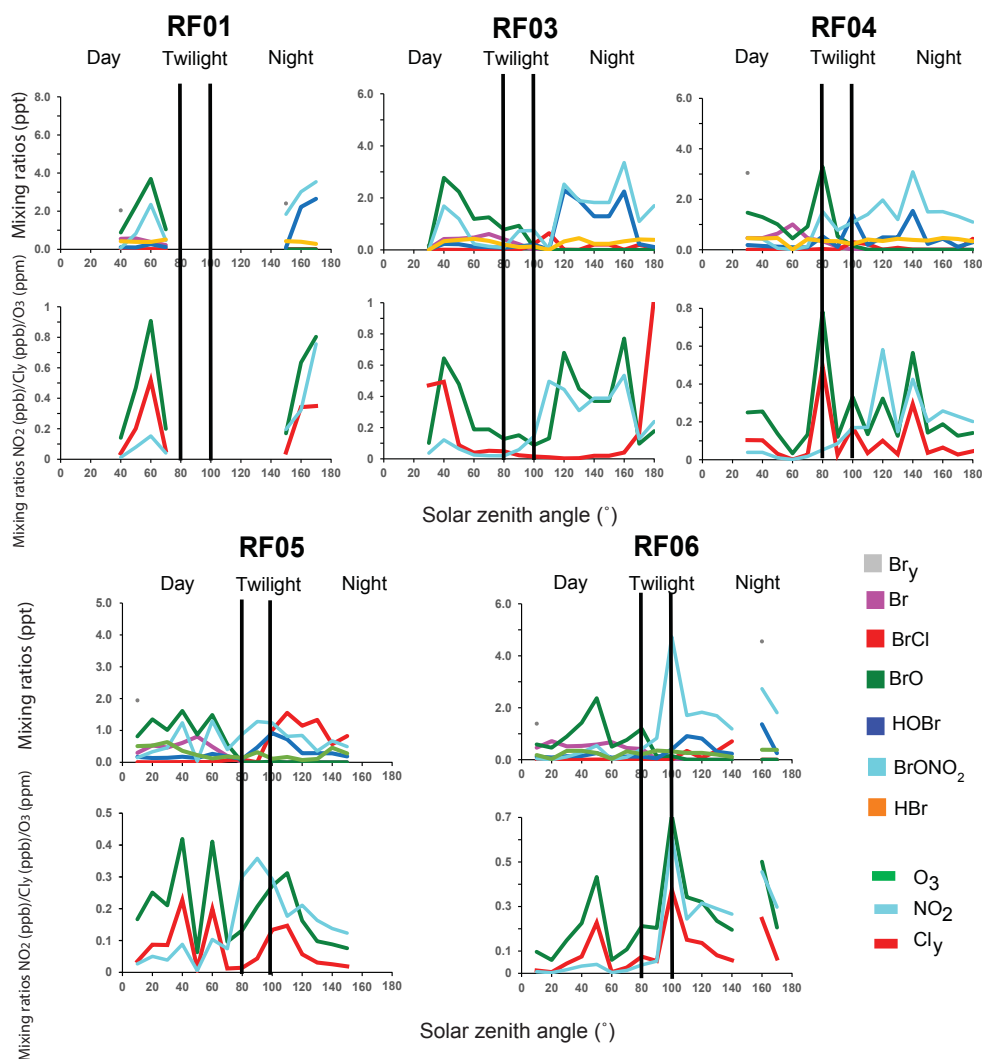
Figure 6. Inorganic bromine species and main reactants of the inorganic chemistry sampled at the same times and locations as the ATTREX flights over the eastern Pacific. Each separate panel show SZA dependent results for flights RF01, RF03, RF04, RF05 and RF06. Only output sampled between 14 and 18 km is considered.

surface areas and lower NO_x levels prevailing over the WP (Fig. 7a).

The scenario over the EP is slightly different as levels of NO_2 and O_3 are higher, while the surface area density of ice crystals (SAD-ICE) is reduced (see Sect. 3.3). A statistical analysis of CAM-Chem NO_2 during daylight over the EP is presented in Fig. 8. Our average range of NO_2 mixing ratios is approximately 15 ± 6 ppt at 14 km, with slightly higher values of 22 ± 24 ppt at 17 km over the tropopause level. These observations made during ATTREX 2013 over the EP agree within 1 standard deviation with the NO_2 values presented by Stutz et al. (2017) and Werner et al. (2017). Their O_3 scaling technique allowed retrieval of NO_2 concentrations of 15 ± 15 ppt in the TTL, with a range of 70–170 ppt in the mid-latitude lower stratosphere associated with older stratospheric air intrusions. However, previous studies have

shown large associated uncertainties in NO_2 measurements based on remote sensing instruments, which also depends on the individual observation geometries and instrument operation times (e.g., 30 % of total relative error of NO_2 measurements below 25 km; Weidner et al., 2005 and 50 % error for satellite measurements from SAGE II bellow 25 km; Bauer et al., 2012).

Hence, the EP daytime average concentrations of ozone (up to ~ 300 ppb), Cl_y (max. ~ 181 ppt), and NO_2 (max. ~ 48 ppt) are almost twice as high as those over the WP (Fig. 7d), while SAD-ICE levels are up to 1 order of magnitude lower (see Fernandez et al., 2014). Higher concentrations of ozone were associated with enhanced production of BrO (Fig. 7c). Meanwhile, during dark hours the higher NO_2 concentrations and the slower rate of heterogeneous reactions of bromine reservoirs (see Sect. 3.3) lead to the for-
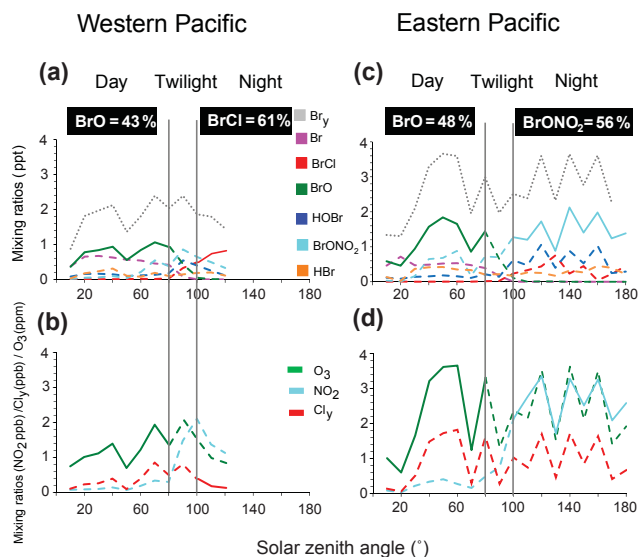
Figure 7. Average of inorganic bromine species **(a, c)** and main reactants of the inorganic chemistry **(b, d)** for all ATTREX flights developed over the western Pacific **(a, b)** and eastern Pacific **(c, d)**. The output from each flight has only been sampled between 14 and 18 km and the average has been performed within $\pm 5°$ SZA bins. Black boxes indicate the percentage of the dominant Br_y species for day and night at 17 km.

Figure 8. Box plot of CAM-Chem NO_2 estimates as a function of altitude during daylight over the eastern Pacific. The filled boxes display the minimum, first quartile (Q1), median (Q2), third quartile (Q3), and maximum values. The black line across the interior of the box represents the median (Q2) of NO_2 for the corresponding altitude. The bottom of the box is the first quartile (Q1) or the 25th percentile; the top of the box is the third quartile (Q3) or the 75th percentile. T bars extending from the boxes represent the largest and the smallest non-outlier values. Circles and stars are the outliers defined according to the interquartile range (IQR = Q3–Q1): circles are the "out values" or the NO_2 mixing ratios greater than 1.5 times the interquartile range, and stars are the "extreme values" or the NO_2 mixing ratios greater than 3 times the interquartile range. The numbers inside the box represent the average NO_2 concentration.

mation of $BrONO_2$ and the reduction of BrCl levels over the EP (Fig. 7c). These results are in good agreement with the partitioning of Br_y found by Werner et al. (2017), where BrO is the dominant daylight species over the EP, and the estimates of Fernandez et al. (2014), which suggest BrO and $BrONO_2$ as the dominant species in the TTL over the entire tropics during daytime and nighttime, respectively.

Note that the predicted differences in Cl_y abundance can reach factors as much as 5 times larger for the EP if individual flights are considered (e.g., max. $Cl_y \sim 500$ ppt for RF01, RF03, and RF04 performed in the EP during ATTREX 2013, while max. Cl_y for all flights (except RF07, less than 400 pptv) remains below 100 ppt). However, the nighttime BrCl abundance is still larger in the WP, representing more than 90 % of the nighttime Br_y partitioning for flights RF02 and RF04 (see Fig. 5). For these cases, BrCl mixing ratios between 1 and 2 pptv are modeled within air parcels with a very low Cl_y abundance (of the order of 6 ppt). In order to understand this unexpected behavior, we performed a sensitivity simulation neglecting the inter-halogen heterogeneous recycling occurring on upper tropospheric ice crystals, see Sect. 3.3 below.

3.2.1 Tropical ring of atomic Br: indications from this case study

Our results also indicate that, integrated over all SZAs, the second most abundant species over both the EP and WP dur-
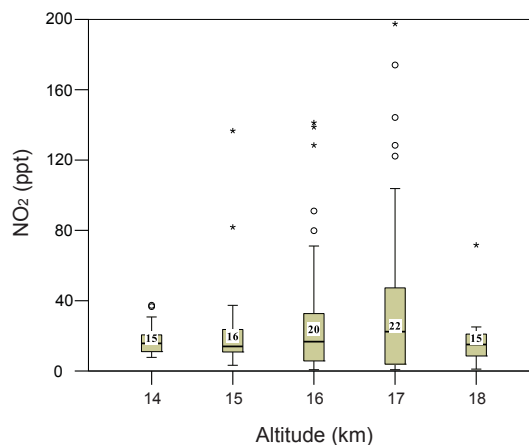
ing daytime is atomic Br. This species plays a fundamental role in the formation of the proposed inhomogeneous tropical ring of atomic Br, a natural atmospheric phenomenon that comes from the rapid photochemical equilibrium between BrO and Br under conditions of low O_3 and low temperatures (Fernandez et al., 2014; Saiz-Lopez and Fernandez, 2016). According to our simulations, during daytime hours the average mixing ratios of Br remain below 0.75 ppt over the EP and WP along the entire range of altitudes (i.e., between 14 and 18 km) (Fig. 4). However, modeled atomic Br abundances surpass BrO mixing ratios at low SZAs (close to noontime) and low ozone abundances (below 100 ppb, Fig. 7b and d). These observations contrast with the variability observed in BrO, which varies from 0.61 to 1.19 ppt over the WP and from 0.72 to 1.43 ppt over the EP (Fig. 4), depending on O_3 and NO_2 background levels. Also, Br shows a smooth variation during the day, slightly decreasing its abundance as the SZA increases, while the temporal evolution of BrO is more variable, mostly under the higher NO_x levels prevailing in the EP (Fig. 7). A closer inspection of each separate flight (Figs. 5 and 6) reveals the large inhomogeneity of the tropical rings of atomic bromine. In the EP, modeled Br surpasses BrO mixing ratios at 60° SZA for flights RF04 and RF06, but as the remaining flights sampled larger BrO mixing ratios the mean EP abundances shown in Fig. 7c show

Br / BrO > 1 only at 20° SZA. Similarly, the mean results shown in Fig. 7a for the WP show BrO > Br at all times, but RF02 and RF03 show the ratio Br / BrO is larger than the one at 50° SZA. This highlights the importance of considering non-averaged (both spatially and temporally) model output to determine the concentration of photochemically reactive species or other atmospheric quantities such as the Br / BrO ratio.

In contrast to the study of Werner et al. (2017), which focused on ATTREX measurements taken over the EP and used an O_3 scaling technique to retrieve their results, our model calculations support the prediction that the Br / BrO ratio could become larger than unity, particularly in the tropical upper troposphere (UT) and TTL of both the eastern and western Pacific Ocean during daylight hours, especially at low SZA. This enhancement of Br atoms in the TTL has also been identified in other studies and seems to be a consistent feature in global models including a complete treatment of halogen chemistry in the troposphere (Chen et al., 2016; Holmes et al., 2006; Schmidt et al., 2016). Nevertheless, the combination of ozone concentrations and temperatures plays a fundamental role in the distribution of both species. Thus, we expect to find a spatially irregular pattern in the conditions that favor Br / BrO > 1.

Figure 9 shows the distribution of the Br / BrO ratio over the WP and EP, and its correlation with ozone concentrations and temperatures. The results in the figure are based on the average 1 km binned data for all track flights, although equivalent conclusions can be drawn for each separate flight transect. Over the EP, Br / BrO > 1 is predicted in discrete air masses, particularly at SZAs between 40° and local noon. Cold temperatures and low O_3 concentrations enhance the prevalence of atomic Br for those times and locations. Indeed, Saiz-Lopez and Fernandez (2016) determined that Br becomes the dominant species for $O_3 < 100$ ppb and $T < 200$ K. Br / BrO ratios lower than 1 are observed near the tropopause for SZAs between 40 and 55° under higher concentrations of ozone and at warmer temperatures. The Br / BrO distribution over the WP seems to be more inhomogeneous with an overall higher Br / BrO ratio than over the EP. The lower ratio of Br / BrO in the EP compared to WP could be due to the higher levels of O_3 modeled in this region (Fig. 2). In any case, the presence of the tropical rings of Br occurs as a patchy distribution of bromine atoms superimposed on a BrO background curtain. In general, the Br / BrO ratio peaks at 17 km, very close to the upper limit of the TTL, highlighting the importance of determining Br abundances in order to address the total amounts of Br_y injected into the stratosphere.

As the magnitude of the Br_y reactive species (Br and BrO) depends on changes in the oceanic sources and vertical transport, the Br / BrO ratio will vary according to season and geographical region. Hence, during strong convective events over the WP (e.g., air masses tracked from the SPCZ) the amount of Br and BrO remained similar to each other. These
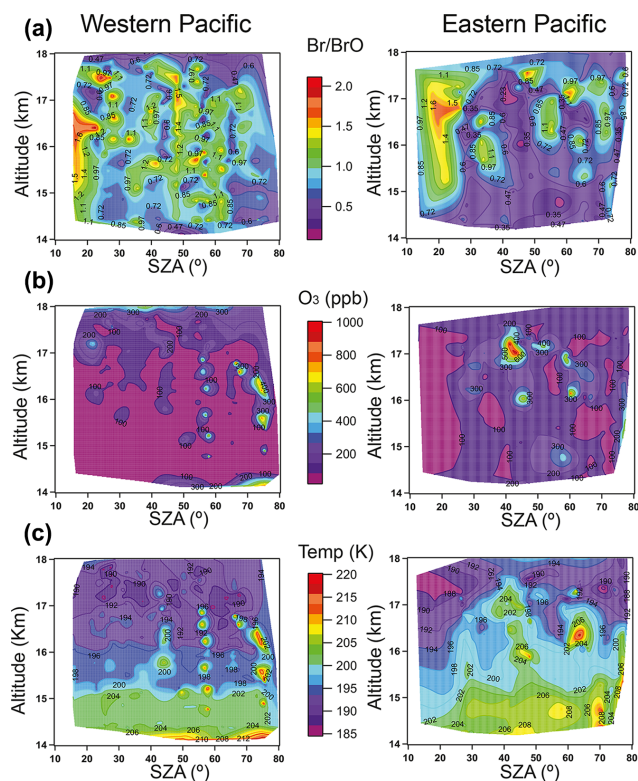

Figure 9. CAM-Chem model estimates of the daylight Br / BrO ratio (**a**), ozone (**b**), and temperature (**c**) as a function of SZA over the WP and EP.
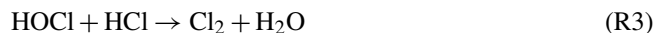
results are in good agreement with Fernandez et al. (2014) who suggested that Br / BrO > 1 during strong convective periods over the WP warm pool region.

Reservoir species like HBr and HOBr were the third most dominant Br_y components. These two species contribute to the formation of BrCl through heterogeneous recycling reactions (see Ordóñez et al., 2012), particularly at night due to the absence of photolysis reactions and the presence of traces of chlorine. As suggested by Fernandez et al. (2014), higher abundances of Cl_y could result from the decomposition of very short-lived chlorocarbons or the subsidence of HCl from the stratosphere to the TTL, driving the nighttime chemistry in areas where $Cl_y > Br_y$.

3.3 Heterogeneous reactions: impact of water–ice recycling on Br_y speciation and distribution

Heterogeneous recycling reactions of reservoir species on ice crystals are relevant at UTLS altitudes. Thus, a sensitivity test was carried out to determine the influence of water-ice aerosols on the partitioning of inorganic species. Reactions (R1) to (R6) show the chlorine, bromine, and interhalogen tropospheric heterogeneous reactions that occur on ice crystals (for a complete description of the implementation of heterogeneous reactions in CAM-Chem, see Table S1 in

the supplementary online material of Fernandez et al., 2014).

$$BrONO_2 \rightarrow HOBr + HNO_3 \qquad (R1)$$

$$ClONO_2 \rightarrow HOCl + HNO_3 \qquad (R2)$$

$$HOCl + HCl \rightarrow Cl_2 + H_2O \qquad (R3)$$

$$HOCl + HBr \rightarrow BrCl + H_2O \qquad (R4)$$

$$HOBr + HCl \rightarrow BrCl + H_2O \qquad (R5)$$

$$HOBr + HBr \rightarrow Br_2 + H_2O \qquad (R6)$$

Including heterogeneous reactions in the chemical mechanism changes the relative partitioning between Br_y species, and consequently the abundance of the dominant species that controls the effective removal is altered. Thus, turning on and off heterogeneous reactions will change the bromine sinks within the UT and TTL, as the relative efficiency of effective washout for each independent Br_y species is different in the model (i.e., individual Henry's law constants are considered for each species). Figure 10 shows mixing ratios at different altitudes when water–ice aerosol reactions were deactivated simultaneously. Relative to the results from the complete mechanism (Fig. 4), at 17 km the absence of ice-crystal reactions increases the total inorganic fraction by 7 and 12 % over the EP during the day and night, respectively. On the other hand, Br_y increases by 29 and 40 % over the WP during day and night, respectively. This relative increase of total Br_y is mainly due to changes in the amount of HBr during the day and an enhancement of both HBr and $BrONO_2$ during the night. As BrCl is only produced by Reactions (4) and (5), it does not accumulate during night hours within the sensitivity study where heterogeneous reactions have been turned off (Fig. 10). The mixing ratios of all other species remain very similar as shown in Figs. 4 and 10. Our model results show that turning off heterogeneous reactions reduces the total amount of Br_y washed out at 17 km by ~ 0.5 and 0.3 pptv for the WP and EP, respectively. This value is of the same magnitude but opposite direction to the results obtained by Aschmann et al. (2011). HBr is highly soluble and it would be expected that a relative increase in HBr partitioning would imply a more efficient washout. However, as explained by Aschmann et al. (2011), it is possible that a significant part of the adsorbed HBr at high altitudes can re-evaporate within the TTL (and eventually reach the stratosphere) before being washed out. This is because the removal process does not occur immediately and residence times are longer in the TTL. Indeed, they found a local HBr maximum at around 17 km within an equivalent sensitivity simulation that neglected heterogeneous activation for HBr.

Another characteristic of the sensitivity test is the clear absence of BrCl during nighttime as water–ice aerosol reactions of HOBr and HCl are suppressed. Compared to the base case, the absence of BrCl makes $BrONO_2$ the dominant species at night over the WP, with 53 % at 17 km compared to 61 % BrCl in the base case. Thus, neglecting ice-recycling Reactions (R1) to (R6) prevents the heterogeneous
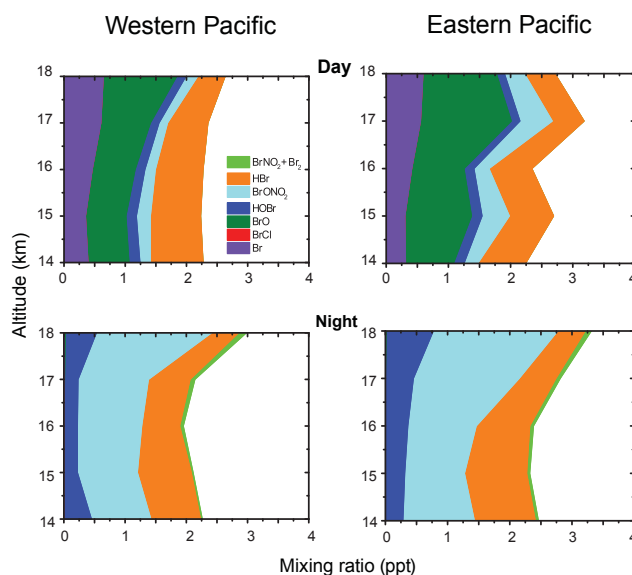

Figure 10. Inorganic bromine partitioning along ATTREX flight tracks over the western and eastern Pacific. Similar to Fig. 4, but ice aerosol recycling reactions in the CAM-Chem chemical mechanism were turned off in this simulation.

conversion of $BrONO_2$ to BrCl, and gas-phase bromine nitrate (which is formed mainly by the termolecular reaction of $BrO + NO_2 + M$, where M is molecule, during twilight) remain as the dominant Br_y species during the night for both the EP and WP regions. But when the heterogeneous recycling reactions are activated, the model predicts that the recycling efficiency depends mostly on the total SAD-ICE prevailing in the upper troposphere. Even under very low Cl_y concentrations (between 10 and 20 ppt), if SAD-ICE is present in the TTL the nighttime reservoir partitioning is shifted to BrCl. Fernandez et al. (2014) found tropospheric SAD-ICE levels within the western Pacific upper TTL to be some of the highest within the tropics, suggesting that BrCl abundance should peak in this region of the Pacific. The smaller impact of turning off heterogeneous reactions in the EP can be explained by the less efficient inorganic bromine recycling occurring on the smaller SAD-ICE prevailing in this region. However, the heterogeneous chemistry of bromine species with water-ice aerosols still requires further research as their atmospheric surfaces are highly dynamic. Indeed, von Hobe et al. (2011) suggested that the coupling of chlorine and nitrogen compounds in the tropical UTLS may not be completely understood, which would also impact on the bromine burden. The presence of cirrus ice clouds, at the cold temperatures of the equatorial and midlatitude UTLS, facilitates the conversion of bromine reservoir species to more photochemically active forms, which play an important role in the oxidative capacity of this region of the atmosphere.

4   Summary and conclusions

Our estimates of Br_y partitioning in the TTL over the Pacific Ocean showed that mostly BrO and to a lesser extent atomic Br are the dominant species during daytime hours, while BrCl and $BrONO_2$ are predicted to dominate the TTL Br_y at nighttime over the WP and EP. The difference in the partitioning of Br_y during the diurnal cycle between the WP and EP could be explained by the changes in the abundance of O_3, NO_2, and Cl_y in these two regions of the Pacific, as well as by the efficiency of heterogeneous reactions that could modify this chemistry, mostly during the night. Table 1 summarizes the results found at 17 km.

Reactive species like atomic Br become the dominant Br_y species in patchy regions of the eastern and western Pacific TTL during daylight, following the large inhomogeneity of ozone abundances within these regions strongly influenced by deep convection. The low ozone concentration and cold conditions, in combination with the rapid photochemical equilibrium between BrO and Br, favor Br / BrO > 1 for patchy regions of the TTL and are consistent with previous results about the proposed tropical rings of atomic bromine. The CAM-Chem output along the ATTREX flights indicates that Br and BrO alternate as the dominant daytime species, indicating a large inhomogeneity for the tropical ring of Br, mainly due to the large ozone and temperature variability of the air parcels within the convective tropical WP and EP. Improved field data for the identification and complete speciation of bromine species are needed to continue evaluating this hypothesis.

This model study contributes to the growing database of reactive halogen estimates based on halocarbon observations. The variable photodecomposition of VSL_{org}, the transport of inorganic degradation products from the lower troposphere into the TTL, and the efficiency of heterogeneous reactions involving ice aerosols play an important role in the overall upper tropospheric Br_y loading and the consequent stratospheric bromine injection. However, further research on the organic/inorganic bromine fraction, as well as its distribution between reactive and reservoir species, is needed in different areas of the globe and at different heights to reduce the uncertainty in the amount of Br_y that enters the stratosphere and to properly constrain the global bromine budget.

Competing interests. The authors declare that they have no conflict of interest.

References

Aschmann, J., Sinnhuber, B.-M., Chipperfield, M. P., and Hossaini, R.: Impact of deep convection and dehydration on bromine loading in the upper troposphere and lower stratosphere, Atmos. Chem. Phys., 11, 2671–2687, https://doi.org/10.5194/acp-11-2671-2011, 2011.

Bauer, R., Rozanov, A., McLinden, C. A., Gordley, L. L., Lotz, W., Russell III, J. M., Walker, K. A., Zawodny, J. M., Ladstätter-Weißenmayer, A., Bovensmann, H., and Burrows, J. P.: Validation of SCIAMACHY limb NO_2 profiles using solar occultation measurements, Atmos. Meas. Tech., 5, 1059–1084, https://doi.org/10.5194/amt-5-1059-2012, 2012.

Blake, N. J., Blake, D. R., Chen, T. Y., Collins, J. E., Sachse, G. W., Anderson, B. E., and Rowland, F. S.: Distribution and seasonality of selected hydrocarbons and halocarbons over the western Pacific basin during PEM-West A and PEM-West B, J. Geophys. Res.-Atmos., 102, 28315–28331, 1997.

Blake, N. J., Blake, D. R., Wingenter, O. W., Sive, B. C., McKenzie, L. M., Lopez, J. P., Simpson, I. J., Fuelberg, H. E., Sachse, G. W., and Anderson, B. E.: Influence of southern hemispheric biomass burning on midtropospheric distributions of nonmethane hydrocarbons and selected halocarbons over the remote South Pacific, J. Geophys. Res.-Atmos., 104, 16213–16232, 1999.

Blake, N. J., Blake, D. R., Simpson, I. J., Lopez, J. P., Johnston, N. A., Swanson, A. L., Katzenstein, A. S., Meinardi, S., Sive, B. C., and Colman, J. J.: Large-scale latitudinal and vertical distributions of NMHCs and selected halocarbons in the troposphere over the Pacific Ocean during the March–April 1999 Pacific Exploratory Mission (PEM-Tropics B), J. Geophys. Res.-Atmos., 106, 32627–32644, 2001.

Blake, N. J., Blake, D. R., Swanson, A. L., Atlas, E., Flocke, F., and Rowland, F. S.: Latitudinal, vertical, and seasonal variations of C1-C4 alkyl nitrates in the troposphere over

the Pacific Ocean during PEM-Tropics A and B: Oceanic and continental sources, J. Geophys. Res.-Atmos., 108, 8242, https://doi.org/10.1029/2001JD001444, 2003.

Blake, N. J., Streets, D. G., Woo, J. H., Simpson, I. J., Green, J., Meinardi, S., Kita, K., Atlas, E., Fuelberg, H. E., and Sachse, G.: Carbonyl sulfide and carbon disulfide: Large-scale distributions over the western Pacific and emissions from Asia during TRACE-P, J. Geophys. Res.-Atmos., 109, D15S05, https://doi.org/10.1029/2003JD004259, 2004.

Brinckmann, S., Engel, A., Bönisch, H., Quack, B., and Atlas, E.: Short-lived brominated hydrocarbons – observations in the source regions and the tropical tropopause layer, Atmos. Chem. Phys., 12, 1213–1228, https://doi.org/10.5194/acp-12-1213-2012, 2012.

Chen, D., Huey, L. G., Tanner, D. J., Salawitch, R. J., Anderson, D. C., Wales, P. A., Pan, L. L., Atlas, E. L., Hornbrook, R. S., and Apel, E. C.: Airborne measurements of BrO and the sum of HOBr and Br_2 over the Tropical West Pacific from 1 to 15 km during the CONvective TRansport of Active Species in the Tropics (CONTRAST) experiment, J. Geophys. Res.-Atmos., 121, 12560–12578, https://doi.org/10.1002/2016JD025561, 2016.

Daniel, J., Solomon, S., Portmann, R., and Garcia, R.: Stratospheric ozone destruction: The importance of bromine relative to chlorine, J. Geophys. Res.-Atmos., 104, 23871–23880, 1999.

Dorf, M., Butz, A., Camy-Peyret, C., Chipperfield, M. P., Kritten, L., and Pfeilsticker, K.: Bromine in the tropical troposphere and stratosphere as derived from balloon-borne BrO observations, Atmos. Chem. Phys., 8, 7265–7271, https://doi.org/10.5194/acp-8-7265-2008, 2008.

Fernandez, R. P., Salawitch, R. J., Kinnison, D. E., Lamarque, J.-F., and Saiz-Lopez, A.: Bromine partitioning in the tropical tropopause layer: implications for stratospheric injection, Atmos. Chem. Phys., 14, 13391–13410, https://doi.org/10.5194/acp-14-13391-2014, 2014.

Fernandez, R. P., Kinnison, D. E., Lamarque, J.-F., Tilmes, S., and Saiz-Lopez, A.: Impact of biogenic very short-lived bromine on the Antarctic ozone hole during the 21st century, Atmos. Chem. Phys., 17, 1673–1688, https://doi.org/10.5194/acp-17-1673-2017, 2017.

Holmes, C. D., Jacob, D. J., and Yang, X.: Global lifetime of elemental mercury against oxidation by atomic bromine in the free troposphere, Geophys. Res. Lett., 33, L20808, https://doi.org/10.1029/2006GL027176, 2006.

Hossaini, R., Chipperfield, M. P., Monge-Sanz, B. M., Richards, N. A. D., Atlas, E., and Blake, D. R.: Bromoform and dibromomethane in the tropics: a 3-D model study of chemistry and transport, Atmos. Chem. Phys., 10, 719–735, https://doi.org/10.5194/acp-10-719-2010, 2010.

Hossaini, R., Chipperfield, M., Montzka, S., Rap, A., Dhomse, S., and Feng, W.: Efficiency of short-lived halogens at influencing climate through depletion of stratospheric ozone, Nat. Geosci., 8, 186–190, https://doi.org/10.1038/ngeo2363, 2015.

Jensen, E. J., Pfister, L., Jordan, D. E., Bui, T. V., Ueyama, R., Singh, H. B., Thornberry, T., Rollins, A. W., Gao, R.-S., and Fahey, D. W.: The NASA Airborne Tropical TRopopause EXperiment (ATTREX): High-altitude aircraft measurements in the tropical western Pacific, B. Am. Meteorol. Soc., 98, 129–143, https://doi.org/10.1175/BAMS-D-14-00263.1, 2015.

Jurkat, T., Voigt, C., Kaufmann, S., Zahn, A., Sprenger, M., Hoor, P., Bozem, H., Müller, S., Dörnbrack, A., and Schlager, H.: A quantitative analysis of stratospheric HCl, HNO_3, and O_3 in the tropopause region near the subtropical jet, Geophys. Res. Lett., 41, 3315–3321, 2014.

Kormann, R., Fischer, H., de Reus, M., Lawrence, M., Brühl, Ch., von Kuhlmann, R., Holzinger, R., Williams, J., Lelieveld, J., Warneke, C., de Gouw, J., Heland, J., Ziereis, H., and Schlager, H.: Formaldehyde over the eastern Mediterranean during MINOS: Comparison of airborne in-situ measurements with 3D-model results, Atmos. Chem. Phys., 3, 851–861, https://doi.org/10.5194/acp-3-851-2003, 2003.

Krysztofiak, G., Catoire, V., Poulet, G., Marécal, V., Pirre, M., Louis, F., Canneaux, S., and Josse, B.: Detailed modeling of the atmospheric degradation mechanism of very-short lived brominated species, Atmos. Environ., 59, 514–532, 2012.

Lamarque, J.-F., Kyle, G. P., Meinshausen, M., Riahi, K., Smith, S. J., van Vuuren, D. P., Conley, A. J., and Vitt, F.: Global and regional evolution of short-lived radiatively-active gases and aerosols in the Representative Concentration Pathways, Climatic Change, 109, 191, https://doi.org/10.1007/s10584-011-0155-0, 2011.

Lamarque, J.-F., Emmons, L. K., Hess, P. G., Kinnison, D. E., Tilmes, S., Vitt, F., Heald, C. L., Holland, E. A., Lauritzen, P. H., Neu, J., Orlando, J. J., Rasch, P. J., and Tyndall, G. K.: CAM-chem: description and evaluation of interactive atmospheric chemistry in the Community Earth System Model, Geosci. Model Dev., 5, 369–411, https://doi.org/10.5194/gmd-5-369-2012, 2012.

Liang, Q., Stolarski, R. S., Kawa, S. R., Nielsen, J. E., Douglass, A. R., Rodriguez, J. M., Blake, D. R., Atlas, E. L., and Ott, L. E.: Finding the missing stratospheric Bry: a global modeling study of $CHBr_3$ and CH_2Br_2, Atmos. Chem. Phys., 10, 2269–2286, https://doi.org/10.5194/acp-10-2269-2010, 2010.

Marcy, T., Fahey, D., Gao, R., Popp, P., Richard, E., Thompson, T., Rosenlof, K., Ray, E., Salawitch, R., and Atherton, C.: Quantifying stratospheric ozone in the upper troposphere with in situ measurements of HCl, Science, 304, 261–265, 2004.

Mébarki, Y., Catoire, V., Huret, N., Berthet, G., Robert, C., and Poulet, G.: More evidence for very short-lived substance contribution to stratospheric chlorine inferred from HCl balloon-borne in situ measurements in the tropics, Atmos. Chem. Phys., 10, 397–409, https://doi.org/10.5194/acp-10-397-2010, 2010.

Meinshausen, M., Smith, S. J., Calvin, K., Daniel, J. S., Kainuma, M. L. T., Lamarque, J. F., Matsumoto, K., Montzka, S. A., Raper, S. C. B., Riahi, K., Thomson, A., Velders, G. J. M., and van Vuuren, D. P. P.: The RCP greenhouse gas concentrations and their extensions from 1765 to 2300, Climatic Change, 109, 213–241, https://doi.org/10.1007/s10584-011-0156-z, 2011.

Navarro, M. A., Atlas, E. L., Saiz-Lopez, A., Rodriguez-Lloveras, X., Kinnison, D. E., Lamarque, J.-F., Tilmes, S., Filus, M., Harris, N. R., and Meneguz, E.: Airborne measurements of organic bromine compounds in the Pacific tropical tropopause layer, P. Natl. Acad. Sci. USA, 112, 13789–13793, 2015.

Neu, J. L. and Prather, M. J.: Toward a more physical representation of precipitation scavenging in global chemistry models: cloud overlap and ice physics and their impact on tropospheric ozone, Atmos. Chem. Phys., 12, 3289–3310, https://doi.org/10.5194/acp-12-3289-2012, 2012.

Olson, J. R., Crawford, J. H., Brune, W., Mao, J., Ren, X., Fried, A., Anderson, B., Apel, E., Beaver, M., Blake, D., Chen, G., Crounse, J., Dibb, J., Diskin, G., Hall, S. R., Huey, L. G., Knapp, D., Richter, D., Riemer, D., Clair, J. St., Ullmann, K., Walega, J., Weibring, P., Weinheimer, A., Wennberg, P., and Wisthaler, A.: An analysis of fast photochemistry over high northern latitudes during spring and summer using in-situ observations from ARCTAS and TOPSE, Atmos. Chem. Phys., 12, 6799–6825, https://doi.org/10.5194/acp-12-6799-2012, 2012.

Oram, D. E., Ashfold, M. J., Laube, J. C., Gooch, L. J., Humphrey, S., Sturges, W. T., Leedham-Elvidge, E., Forster, G. L., Harris, N. R. P., Mead, M. I., Abu Samah, A., Phang, S. M., Chang-Feng, O.-Y., Lin, N.-H., Wang, J.-L., Baker, A. K., Brenninkmeijer, C. A. M., and Sherry, D.: A growing threat to the ozone layer from short-lived anthropogenic chlorocarbons, Atmos. Chem. Phys. Discuss., https://doi.org/10.5194/acp-2017-497, in review, 2017.

Ordóñez, C., Lamarque, J.-F., Tilmes, S., Kinnison, D. E., Atlas, E. L., Blake, D. R., Sousa Santos, G., Brasseur, G., and Saiz-Lopez, A.: Bromine and iodine chemistry in a global chemistry-climate model: description and evaluation of very short-lived oceanic sources, Atmos. Chem. Phys., 12, 1423–1447, https://doi.org/10.5194/acp-12-1423-2012, 2012.

Prather, M. J. and Watson, R. T.: Stratospheric ozone depletion and future levels of atmospheric chlorine and bromine, Nature, 344, 729–734, 1990.

Saiz-Lopez, A. and Fernandez, R. P.: On the formation of tropical rings of atomic halogens: Causes and implications, Geophys. Res. Lett., 43, 2928–2935, 2016.

Salawitch, R. J., Weisenstein, D. K., Kovalenko, L. J., Sioris, C. E., Wennberg, P. O., Chance, K., Ko, M. K., and McLinden, C. A.: Sensitivity of ozone to bromine in the lower stratosphere, Geophys. Res. Lett., 32, L05811, https://doi.org/10.1029/2004GL021504, 2005.

Schmidt, J. A., Jacob, D., Horowitz, H., Hu, L., Sherwen, T., Evans, M. J., Liang, Q., Suleiman, R. M., Oram, D., and Le Breton, M.: Modeling the observed tropospheric BrO background: Importance of multiphase chemistry and implications for ozone, OH, and mercury, J. Geophys. Res.-Atmos., 121, 11819–11835, https://doi.org/10.1002/2015JD024229, 2016.

Schroeder, J. R., Pan, L. L., Ryerson, T., Diskin, G., Hair, J., Meinardi, S., Simpson, I., Barletta, B., Blake, N., and Blake, D. R.: Evidence of mixing between polluted convective outflow and stratospheric air in the upper troposphere during DC3, J. Geophys. Res.-Atmos., 119, 11477–11491, https://doi.org/10.1002/2014JD022109, 2014.

Sinnhuber, B.-M., Sheode, N., Sinnhuber, M., Chipperfield, M. P., and Feng, W.: The contribution of anthropogenic bromine emissions to past stratospheric ozone trends: a modelling study, Atmos. Chem. Phys., 9, 2863–2871, https://doi.org/10.5194/acp-9-2863-2009, 2009.

Stutz, J., Werner, B., Spolaor, M., Scalone, L., Festa, J., Tsai, C., Cheung, R., Colosimo, S. F., Tricoli, U., Raecke, R., Hossaini, R., Chipperfield, M. P., Feng, W., Gao, R.-S., Hintsa, E. J., Elkins, J. W., Moore, F. L., Daube, B., Pittman, J., Wofsy, S., and Pfeilsticker, K.: A new Differential Optical Absorption Spectroscopy instrument to study atmospheric chemistry from a high-altitude unmanned aircraft, Atmos. Meas. Tech., 10, 1017–1042, https://doi.org/10.5194/amt-10-1017-2017, 2017.

von Hobe, M., Grooß, J.-U., Günther, G., Konopka, P., Gensch, I., Krämer, M., Spelten, N., Afchine, A., Schiller, C., Ulanovsky, A., Sitnikov, N., Shur, G., Yushkov, V., Ravegnani, F., Cairo, F., Roiger, A., Voigt, C., Schlager, H., Weigel, R., Frey, W., Borrmann, S., Müller, R., and Stroh, F.: Evidence for heterogeneous chlorine activation in the tropical UTLS, Atmos. Chem. Phys., 11, 241–256, https://doi.org/10.5194/acp-11-241-2011, 2011.

Weidner, F., Bösch, H., Bovensmann, H., Burrows, J. P., Butz, A., Camy-Peyret, C., Dorf, M., Gerilowski, K., Gurlit, W., Platt, U., von Friedeburg, C., Wagner, T., and Pfeilsticker, K.: Balloon-borne limb profiling of UV/vis skylight radiances, O_3, NO_2, and BrO: technical set-up and validation of the method, Atmos. Chem. Phys., 5, 1409–1422, https://doi.org/10.5194/acp-5-1409-2005, 2005.

Werner, B., Stutz, J., Spolaor, M., Scalone, L., Raecke, R., Festa, J., Colosimo, S. F., Cheung, R., Tsai, C., Hossaini, R., Chipperfield, M. P., Taverna, G. S., Feng, W., Elkins, J. W., Fahey, D. W., Gao, R.-S., Hintsa, E. J., Thornberry, T. D., Moore, F. L., Navarro, M. A., Atlas, E., Daube, B. C., Pittman, J., Wofsy, S., and Pfeilsticker, K.: Probing the subtropical lowermost stratosphere and the tropical upper troposphere and tropopause layer for inorganic bromine, Atmos. Chem. Phys., 17, 1161–1186, https://doi.org/10.5194/acp-17-1161-2017, 2017.

Wofsy, S. C., McElroy, M. B., and Yung, Y. L.: The chemistry of atmospheric bromine, Geophys. Res. Lett., 2, 215–218, 1975.